Available online at www.sciencedirect.com
SCIENCE DIRECT®

Journal of the European Ceramic Society 24 (2004) 3367–3375
www.elsevier.com/locate/jeurceramsoc

Reaction sintering of fluorine-doped $MgSiN_2$

Z. Lenčéš[a,b,*], K. Hirao[a], S. Kanzaki[a], M.J. Hoffmann[b], P. Šajgalík[c]

[a]*National Institute of Advanced Industrial Science and Technology, Moriyama-ku, Nagoya 463-8687, Japan*
[b]*Institut für Keramik im Maschinenbau, Universität Karlsruhe, Haid-und-Neu-Str. 7, 761 31 Karlsruhe, Germany*
[c]*Institute of Inorganic Chemistry, Slovak Academy of Sciences, Dúbravská cesta 9, 845 36 Bratislava, Slovakia*

Abstract

Reaction bonded $MgSiN_2$ (RBMSN) with CaF_2 and YbF_3, as sintering additives was prepared by direct nitridation of $Si/Mg_2Si/Mg/Si_3N_4$ powder compact in a temperature range 1350–1550 °C. The influence of the ratio of constituents on the final phase composition, the amount of sintering additives and the influence of sintering temperature are discussed. It was shown that the starting powders should be in a ratio $Mg_2Si/Mg \geqslant 3$ and $Si_3N_4/Si_{tot} \geqslant 0.5$ respectively, to obtain single-phase $MgSiN_2$. The oxygen content of $MgSiN_2$ was in the range of 0.4–0.7 wt.%. The final density of pressureless sintered RBMSN with 4 vol.% fluorine additives was 85% of theoretical density. Higher density (~92%) was obtained for the reaction-bonded composite consisting of 48 vol.% $MgSiN_2$ and 52 vol.% Si_3N_4, due to the volume increase after the nitridation of silicon. The mechanical properties of fluorine-doped RBMSN were further improved by hot-pressing at 1600 °C. The 4-point bending strength and Vickers hardness (HV1) of hot-pressed materials are 427 MPa and 20.8 GPa, respectively. The indentation fracture toughness is 5.3 MPa $m^{1/2}$, due to the presence of elongated β-Si_3N_4 grains. The thermal conductivity of the dense reaction bonded $MgSiN_2$ is 22 W $m^{-1}K^{-1}$.

Keywords: Hardness; $MgSiN_2$; Nitrides; Sintering; Strength; Thermal properties

1. Introduction

Magnesium silicon nitride ($MgSiN_2$) is intensively studied in the recent years, as an alternative material for the substrates of the integrated circuits. Although the calculated thermal conductivity of $MgSiN_2$ is 75 W $m^{-1}K^{-1}$,[1] the reported experimental values are in the range 17–25 W $m^{-1}K^{-1}$.[2–5] An improvement in thermal conductivity is expected from the optimisation of the processing route, especially by decreasing the oxygen content in the final product. Except of good thermal conductivity and high electrical resistance, $MgSiN_2$ has high hardness (20 GPa), reasonable strength (280 MPa), and fracture toughness (3 MPa $m^{1/2}$), which makes it suitable for some engineering applications.

Several synthesis procedures have been utilized to prepare $MgSiN_2$. With a conventional synthesis starting with a Mg_3N_2/Si_3N_4 or Mg/Si_3N_4 mixture, $MgSiN_2$ powder with 1–4 wt.% oxygen was produced.[6] $MgSiN_2$ powders prepared by direct nitridation of a Mg/Si mixture always contained free silicon. Single-phase $MgSiN_2$ with low oxygen content (0.76 mol%) was successfully prepared by nitridation of Mg_2Si.[7] The disadvantage of this method is the high excess of magnesium in the starting powder.

The aim of this work is to produce bulk $MgSiN_2$ ceramic material with improved mechanical properties and with low oxygen content from a complex mixture of Mg, Mg_2Si, Si and Si_3N_4 starting powders. Both the reaction bonding process and hot-pressing method are used for densification, together with the addition of CaF_2, YbF_3, and Yb_2O_3, as nitridation promoters and sintering additives. Fluorine based additives were selected, because CaF_2 is an excellent nitridation promoter, as it was observed in the synthesis of AlN powder by the carbothermal reduction-nitridation of Al_2O_3 powder,[8,9] or during the synthesis of $MgSiN_2$ from $MgSiO_3$.[10]

2. Experimental

The starting powder compositions were calculated according to the following general reaction:[11]

* Corresponding author. Tel.: +421-2-52941-0408; fax: +421-7-52941-0444.
E-mail address: uachlenc@savba.sk (Z. Lenčéš).

0955-2219/$ - see front matter © 2003 Elsevier Ltd. All rights reserved.
doi:10.1016/j.jeurceramsoc.2003.10.022

$$(1-2y)\ \mathrm{Mg} + y\ \mathrm{Mg_2Si} + (1-3x-y)\ \mathrm{Si} + x\mathrm{Si_3N_4} + (1-2x)\ \mathrm{N_2} = \mathrm{MgSiN_2} \quad (1)$$

where $0 \leqslant x \leqslant 1/3$ and $0 \leqslant y \leqslant 1–1.5x$. Appropriate amounts of Mg_2Si (Kojundo Chem. Lab., Japan), α-Si_3N_4 (SN-E05, Ube Industries Ltd., Japan), Si (Kojundo Chem. Lab.), and Mg (Mg-100, Yamaishi Metal Co., Japan) powders were mixed in Si_3N_4 pot using planetary ball mill in $N_2 + Ar$ atmosphere. The optimised starting powders composition is described elsewhere.[11] Briefly, it was shown that the total silicon ($Si_{tot} = Si + 0.366Mg_2Si$) and magnesium content in the starting powder should not exceed the ratio $Mg_2Si/Mg \geqslant 3$ and $Si_3N_4/Si_{tot} \geqslant 0.5$, to obtain single-phase $MgSiN_2$. Some powder batches were mixed in a ratio to have 48 vol.% $MgSiN_2$ and 52 vol.% Si_3N_4 in the product (see Table 1). CaF_2, YbF_3 (Wako Pure Chem., Japan) and Yb_2O_3 (Nihon Yttrium, Japan) were used as nitridation promoters and sintering additives in a total amount of 4 vol.%.

Pellets were pressed from the powders in a steel die using 100 MPa pressure. Samples for pressure-less sintering or gas-pressure sintering were also cold isostatically pressed (CIP) using 400 MPa pressure. The samples were nitrided in BN crucible filled with $MgSiN_2 + BN$ powder bed using alumina-tube furnace and sintered or hot-pressed in a graphite resistance furnace at temperatures shown in Table 1. Differential thermal analysis (DTA) and thermogravimetry (TG) were conducted (Model TG 8120, Rigaku, Japan) in flowing nitrogen-gas atmosphere to optimise the nitridation and sintering process. The phase composition was investigated using powder X-ray diffraction (Model RINT2500, Rigaku Co., Japan). The oxygen and nitrogen content was also determined (Model TC-436, LECO, USA). Field emission scanning electron microscopy (Model JSM-6320FK, JEOL, Japan) was used to observe the microstructure. Hardness and fracture toughness were determined using Vickers indentation method (Model AVK-C1, Akashi Co., Japan).[12] The Young's modulus was measured using the pulse-echo method. Thermal diffusivity and specific heat data were obtained using a laser-flash technique (Model TC-7000, Shinku-Riko, Japan). The thermal conductivity, κ, was calculated using the following equation:

$$\kappa = a\rho C_v \quad (2)$$

where a is the thermal diffusivity, ρ is the density, and C_v is the heat capacity at constant volume. The relative dielectric constant, ϵ, has been measured on the ceramic pellets (thickness 1.4 mm, diameter 16 mm) at room temperature using a HP 4284A Precision LCR meter. On both sides of the samples a thin gold layer was deposited by sputtering (4 min). The measurements were performed between 100 Hz and 1 MHz.

Table 1
Composition and heat treatment of $MgSiN_2$-based samples

Sample	$MgSiN_2$ (vol%)	Si_3N_4 (vol%)	Additives (vol%)	Sintering method[a]	Nitrid. (°C/h)	Sinter. (°C/h)
M-P1	100			PLS	1380/1	1500/2
M-P2	48	52		PLS	1380/1	1500/2
M-P3	46	50	4[b]	PLS	1380/1	1500/2
M-G1	46	50	4[b]	GPS	1380/1	1500/2
M-G2	46	50	4[c]	GPS	1380/1	1500/2
M-H0	46	50	4[b]	HP	1380/1	1500/2
M-H1	96		4[b]	HP	1380/1	1530/2
M-H2	46	50	4[c]	HP	1380/1	1530/2
M-H3	46	50	4[b]	HP	1380/1	1530/2
M-G3	46	50	4[c]	GPS	1380/1	1530/2

[a] PLS: pressure-less sintering, GPS: gas-pressure sintering HP: hot pressing.
[b] $YbF_3 + Yb_2O_3$.
[c] $YbF_3 + Yb_2O_3 + CaF_2$.

3. Results and discussion

3.1. Density and microstructure

Fig. 1 shows the TG–DTA curves of sample M-P2. In addition to the strong exothermic peak at 930 °C, three weak exothermic effects at 580, 635, and 1225 °C are observed. The peaks at 575 and 635 °C are attributed to the direct nitridation of Mg to form Mg_3N_2, promoted by the presence of silicon (first peak) and Si_3N_4 (second peak).[6,7] The weight gain on the TG curve to the main exothermic reaction at ~930 °C is due to the formation of Mg_3N_2 (Fig. 1), which was confirmed by XRD analysis. The remarkable increase of weight at 930 °C is due to the nitridation of in-situ formed silicon,[11] and simultaneous formation of $MgSiN_2$. The weak exothermic peak at 1225 °C is connected with the exothermic nitridation of coarser unreacted silicon.

Utilizing the DTA–TG results for the nitridation schedule, the local overheating of samples due to the exothermic effects was successfully avoided during heat treatment. However, the final density of additive-free reaction bonded $MgSiN_2$ was only 72% of the theoretical one. The low density is due to the fact that the nitridation of magnesium is accompanied by volume contraction $\Delta V = -11.2\%$ (see Mg_3N_2 in Fig. 2). On the other hand, after nitridation of silicon the volume increases by +21.6%. Using Mg_2Si and Si_3N_4 or Mg_2Si and silicon as starting powders for the preparation of $MgSiN_2$, the volume contracts by −5.5%, or only by −0.74%. However, with increasing the portion of silicon in the starting powder, also the time of nitridation increases. In this work the condition $Si_3N_4/Si_{tot} \geqslant 0.5$ was fulfilled in all starting powder batches. Additionally,

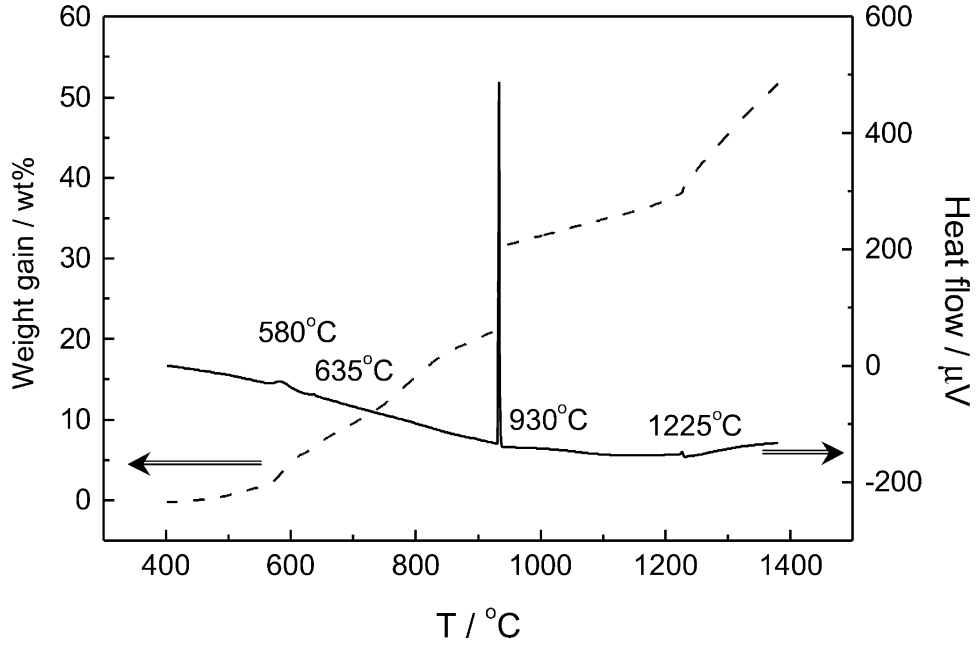

Fig. 1. TG–DTA curves of sample M-P2.

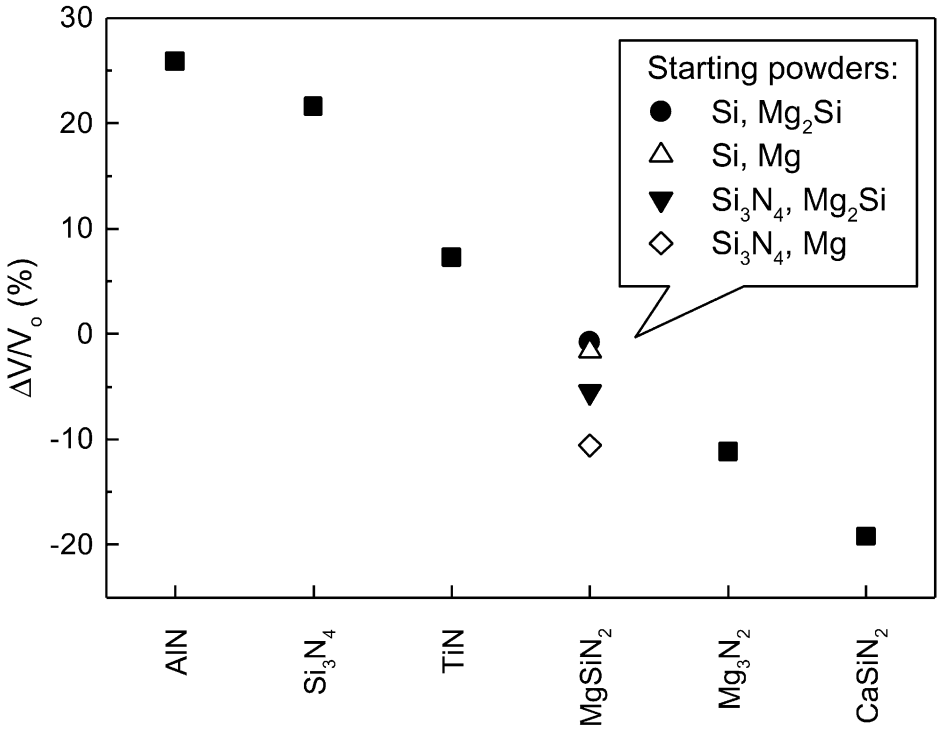

Fig. 2. Volume changes of some elements after their nitridation. The volume change depends on the type of starting powders, as it is shown in the case of $MgSiN_2$.

it was necessary to mill the Mg_2Si starting powder with an average particle size $d \leqslant 150$ μm, because after nitridation large pores were formed in the vicinity of Mg_2Si platelets (Fig. 3). Known the volume changes after nitridation, it was reasonable to combine the reaction bonding of $MgSiN_2$ and Si_3N_4. Sample prepared from $Si/Mg_2Si/Mg/Si_3N_4$ powders with a final composition 48 vol.% $MgSiN_2$ and 52 vol.% Si_3N_4 should have a theoretical volume increase of ~8%. The final density of this reaction bonded composite was 82%, which increased to 94% using $CaF_2 + YbF_3 + Yb_2O_3$ sintering additives, and 0.6 MPa nitrogen pressure (GPS). Samples hot pressed under 30 MPa pressure were fully dense. The beneficial effect of the fluorine additives is

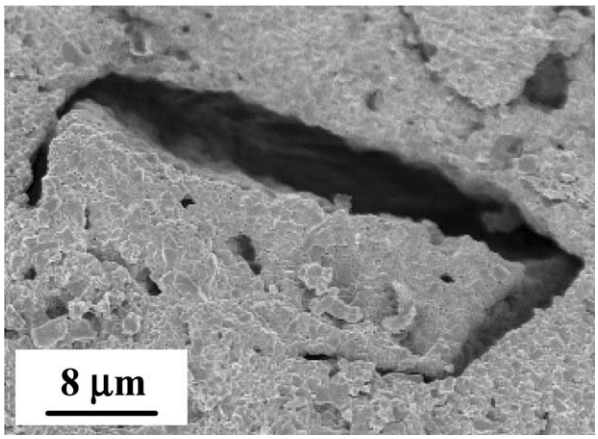

Fig. 3. SEM micrograph of the large Mg_2Si particle after nitridation. The volume contraction is clearly visible.

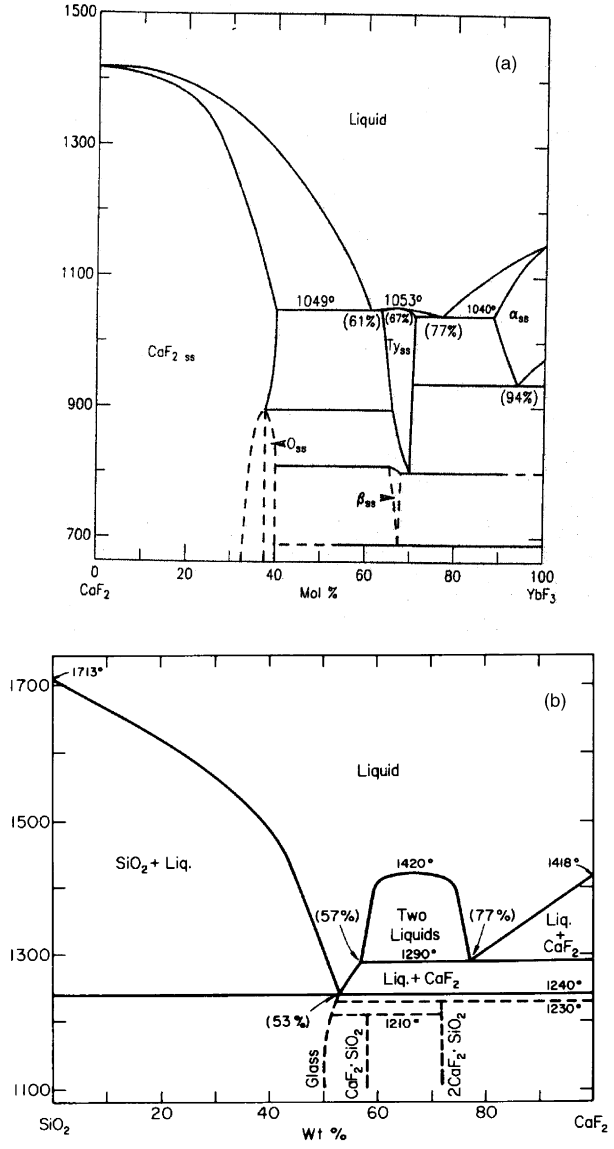

Fig. 4. Phase diagrams of (a) CaF_2–YbF_3, and (b) SiO_2–CaF_2 systems.[13,14]

owing to the formation of liquid phase (see Fig. 4,[13,14]) close to the temperature of $MgSiN_2$ formation (930 °C). Although the YbF_3–Yb_2O_3 phase diagram is not available, it can be estimated that the eutectic temperature is close to the similar YF_3–Y_2O_3 system, which has an eutectic temperature 1125 °C.[15] Moreover, during heat treatment also MgF_2 can be formed (see below Fig. 5), and the eutectic temperature of MgF_2–YbF_3 system is 967 °C.[16] It can be assumed that the liquid-phase formation in the complex system SiO_2–MgO–CaF_2–YbF_3–MgF_2–Yb_2O_3 is close to the above mentioned 930 °C. The liquid phase accelerates the nitridation of silicon at this low temperature. The diffusion of nitrogen and the supersaturation of liquid phase by nitrogen are faster in the low viscous fluorine-based liquid phase, promoting the formation of Si_3N_4 and $MgSiN_2$. To avoid the remarkable loss of magnesium from the reaction system, it is important to finish the nitridation of silicon at temperatures close to the formation of $MgSiN_2$, i.e. at ~930 °C.[11]

It can be concluded that fluorides are effective nitridation promoters and sintering additives for the preparation of dense $MgSiN_2$. Moreover, YbF_3 can contribute to the removal of oxide impurities from the surface of starting powders (Si, Si_3N_4, and Mg_2Si) according to the following reactions:

$$1/2SiO_2(s) + 2/3YbF_3(s,l) = 1/2SiF_4(g) + 1/3Yb_2O_3(s) \quad (3)$$

$$MgO(s) + 2/3YbF_3(s,l) = MgF_2(g) + 1/3Yb_2O_3(s) \quad (4)$$

The standard free energy changes $\Delta_r G°$ of these reactions show that the reduction of SiO_2 proceeds spontaneously in the presence of YbF_3 from 1000 K, while MgO is reduced even at lower temperatures (Fig. 5). Because the standard free energy of formation $\Delta_f G$ of CaF_2 is more negative compared with YbF_3 and MgF_2, it will not reduce their oxides and will act only as sintering aid (Fig. 4b). The beneficial effect of reactions (3) and (4) is the formation of more stable oxide Yb_2O_3, compared with MgO and SiO_2. Consequently, the incorporation of oxygen into the $MgSiN_2$ lattice will decrease. It is well known that the lattice oxygen significantly decreases the thermal conductivity. The thermal conductivities of reaction bonded and hot pressed samples are summarised in Table 2. The highest value is 21.9 W $m^{-1}K^{-1}$ for sample M-H1, slightly lower than 26.6 W $m^{-1}K^{-1}$ reported for $MgSiN_2$ with 1 wt.% Yb_2O_3 addition.[17] It should be mentioned that the samples were nitrided in alumina tube furnace and in this step the reduction of oxygen was limited by the oxygen partial pressure present in the reaction atmosphere. The oxygen content of the samples finally sintered

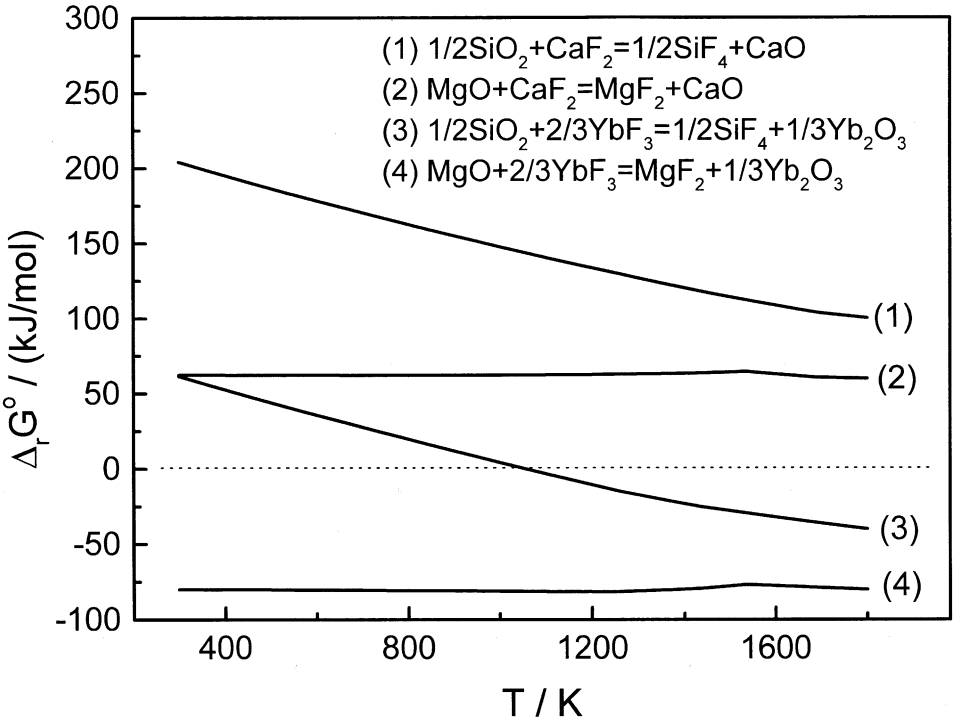

Fig. 5. Temperature dependence of the standard Gibbs free energy of reactions of fluorides with oxide impurities.

Table 2
Thermal and mechanical properties of $MgSiN_2$ samples[a]

Sample	C_p	a	κ	ϵ	Tan δ
	($J\ kg^{-1}K^{-1}$)	(m^2s^{-1})	($W\ m^{-1}K^{-1}$)		
M-H1	760	9.12×10^{-6}	21.9	9.0	0.006
M-H2	680	8.45×10^{-6}	18.3		
M-H3	710	8.16×10^{-6}	18.5		
M-G3	710	8.22×10^{-6}	18.7	44.7	0.07

[a] C_p, heat capacity; a, thermal diffusivity; κ, thermal conductivity; ϵ, dielectric constant (at 100 kHz).

in the graphite resistance furnace, and without Yb_2O_3 addition, was in the range 0.4–0.5 wt.%. As the maximum solubility of oxygen in the $MgSiN_2$ lattice does not exceed 0.5 wt.%,[6] nearly all the oxygen can be dissolved in the $MgSiN_2$ lattice, having a detrimental effect on the thermal conductivity. The composite samples $MgSiN_2 + Si_3N_4$ had lower thermal conductivity, $\sim$18.6 $Wm^{-1}K^{-1}$ (Table 2), most probably owing to the higher dislocation density within the grains, formed as a consequence of the thermal expansion mismatch between $MgSiN_2$ and Si_3N_4. The linear thermal expansion coefficient of $MgSiN_2$ is 7.11×10^{-6} K^{-1}, whereas for Si_3N_4 it is only 3.59×10^{-6} K^{-1} at 1200 K.[18]

The $MeF_x(g)$ side products of reactions (3) and (4) is deposited on the cold part of the furnace, apart from the specimen itself, partly reducing the fluoride impurity, which has a detrimental effect on the high temperature properties of ceramics.[19]

The relative dielectric constant of $MgSiN_2$ with fluorine-based additives is 9.0 at 100 kHz (Table 2), close to the value 10.5 reported by Groen et al.[2] The loss tangent of sample M-H1 is 0.006. The gas-pressure sintered composite sample $MgSiN_2 + Si_3N_4$ has higher dielectric constant 44.7, it even has 3–4 vol.% residual porosity. The dielectric properties of samples M-H2 and M-H3 were not evaluated.

3.2. Microstructure, mechanical and thermal properties

The microstructure of hot-pressed and CF_4/O_2 plasma-etched samples is shown in Fig. 6 a. The elongated β-Si_3N_4 grains, which were added as seeds, and fine α-Si_3N_4 particles are visible after 1 min plasma etching. The unetched area is $MgSiN_2$, as it results from the combination of XRD (Fig. 7) and EDS measurements. Even 9 min plasma etching failed in achieving well-etched $MgSiN_2$ surface. Fig. 6b shows the fracture surface of liquid-phase sintered $MgSiN_2$. The grain size is in the range 0.5–3.0 μm.

In the case of porous samples sintered at 1500 °C for 2 h only the Vickers hardness was measured (Fig. 8). With increasing density the hardness increases, as it was expected. The mechanical properties of dense samples are summarised in Figs. 9 and 10. The monolithic $MgSiN_2$ (sample M-H1) has the highest Vickers hardness 20.8 GPa, similar to 20.7 GPa obtained for the $MgSiN_2$ densified with 1 wt.% Er_2O_3 additive.[17] The Young's modulus of $MgSiN_2$ is 288 GPa, and it increases accordingly for the composite samples, because the

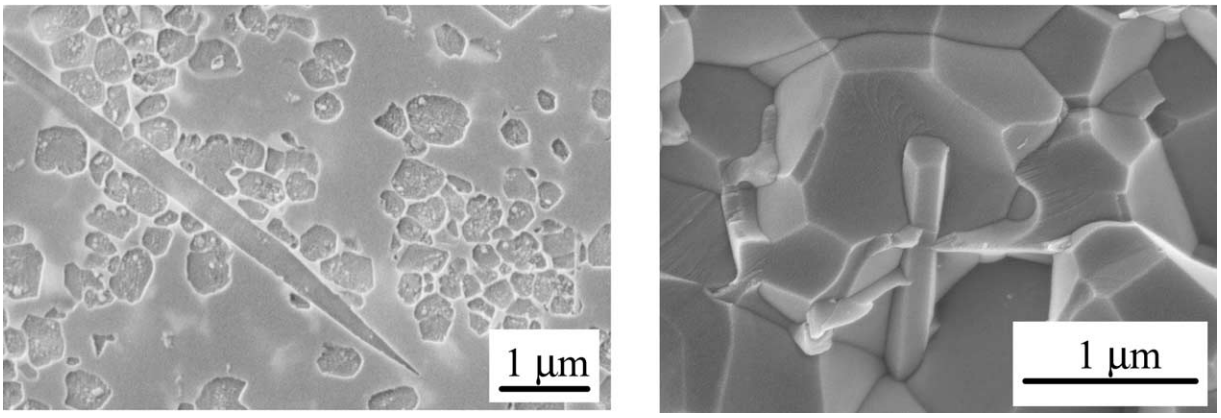

Fig. 6. SEM micrographs of sample M-H2; (a) polished and plasma etched surface, (b) fracture surface of $MgSiN_2$ matrix with elongated β-Si_3N_4 grain.

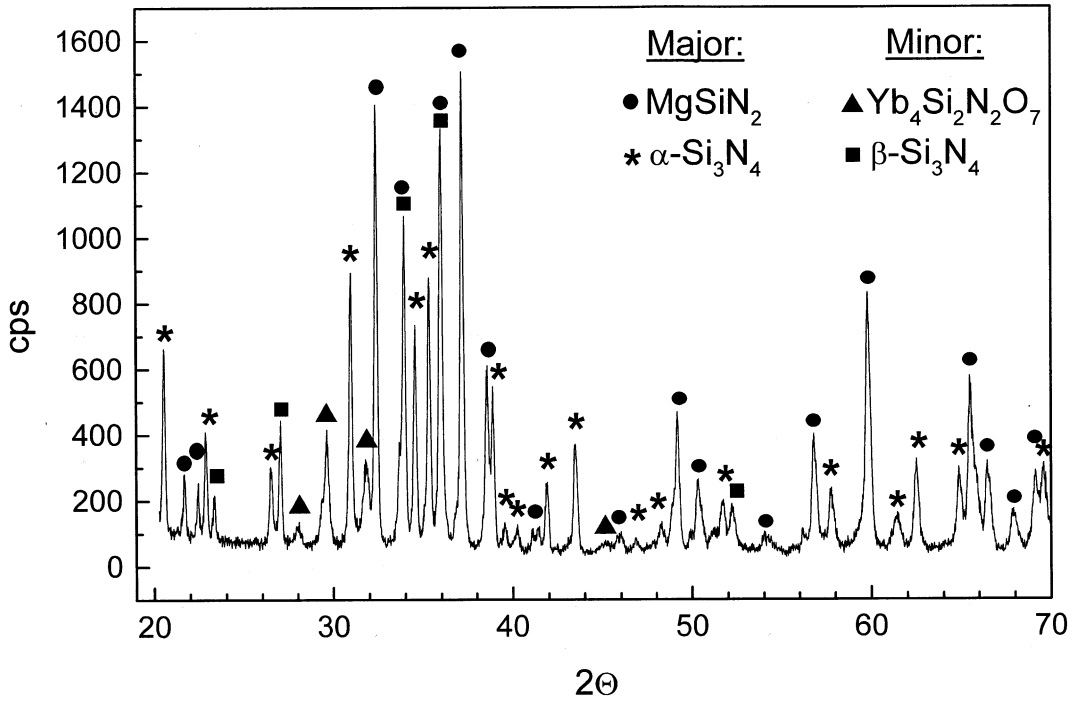

Fig. 7. XRD powder diffractogram of sample M-H2.

elastic modulus of Si_3N_4 is 320 GPa. The composite samples $MgSiN_2 + Si_3N_4$ have also higher strength and fracture toughness (Fig. 10) due to the bimodal microstructure, as shown in Fig. 6a. Sample M-H2 containing also CaF_2 additive has the highest fracture toughness $K_{IC} = 5.3$ MPa $m^{1/2}$, while sample M-H3 with only Yb-based additives has higher bending strength, 427 MPa. The results indicate that samples with CaF_2 additive have weaker grain boundary phase. Kleebe et al.[19] reported that within a certain range of fluorine amount in the grain boundary phase (0.1 wt.% F), the work of fracture displays a noticeable increase and rising R-curve behaviour. On the other hand, even a small amount of fluorine dopant reduced the effective viscosity of the glass and caused more than one order of magnitude increase in creep rate.[20] However, the purpose of this work was not the development of $MgSiN_2$-based material for high-temperature applications.

The mechanical properties of $MgSiN_2$ can be further optimised by grain boundary engineering and microstructure control, similar to those processes applied for the preparation of liquid-phase sintered Si_3N_4 or AlN.

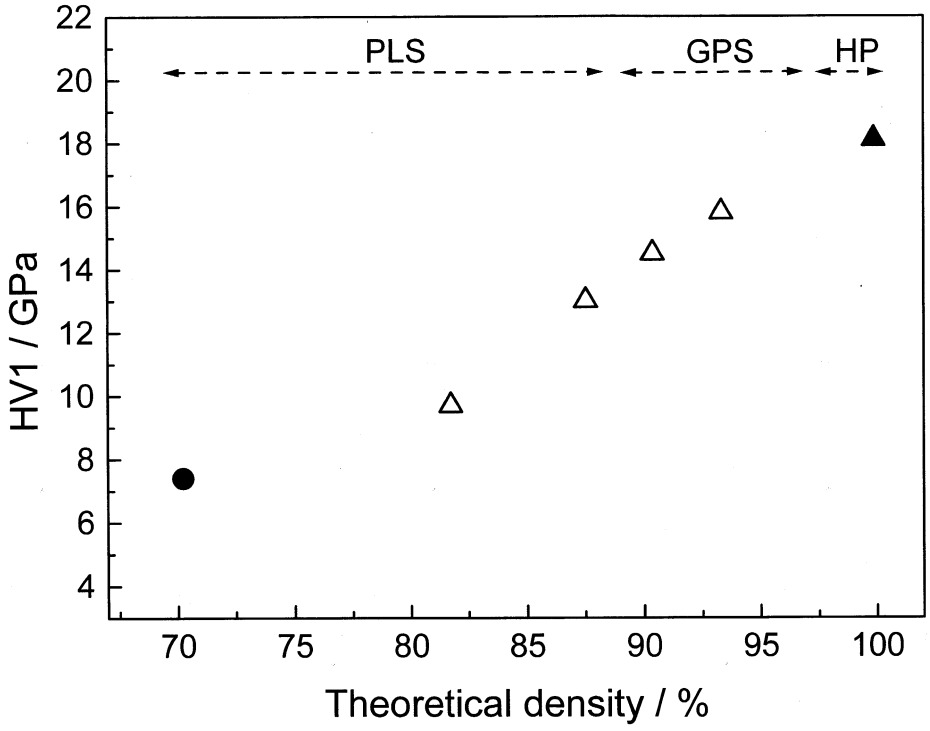

Fig. 8. Vickers hardness as a function of density of samples sintered at 1500 °C/2 h. (●) Sample M-P1; (△) samples M-P2, M-P3, M-G1 and M-G2; (▲) sample M-H0.

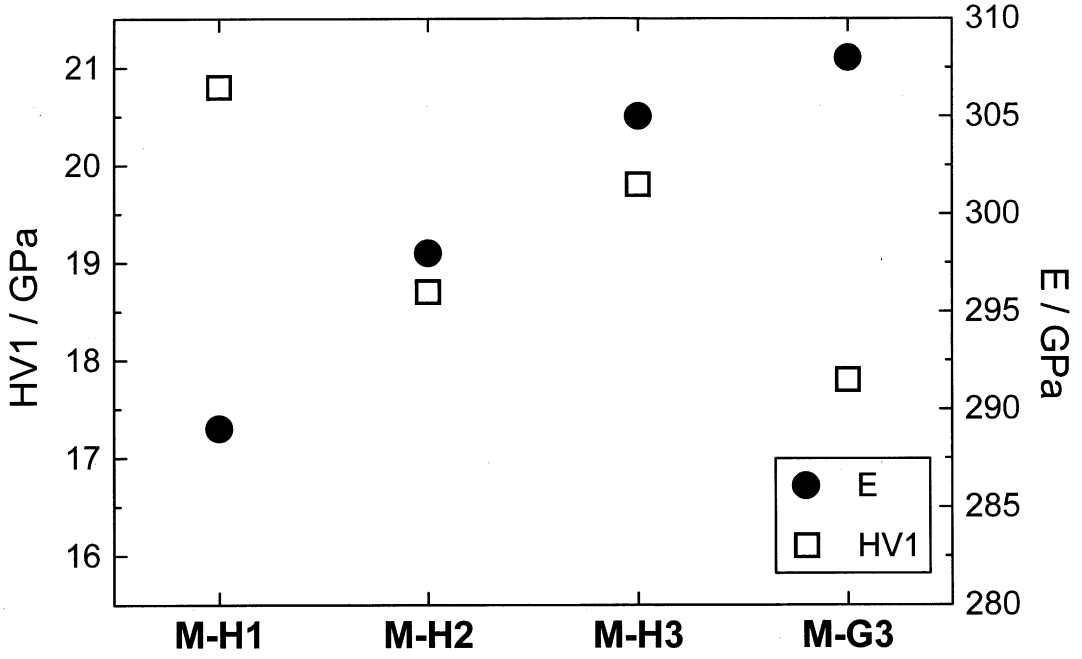

Fig. 9. Vickers hardness (9.81N) and Young's modulus of dense $MgSiN_2$-based samples.

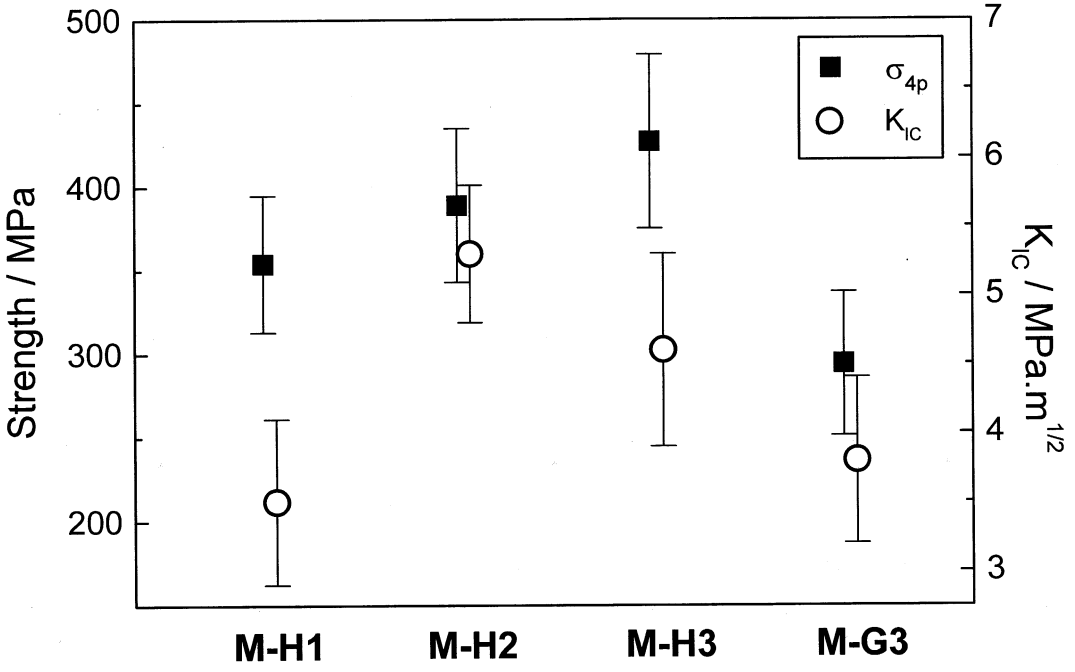

Fig. 10. Four-point bending strength (σ_{4p}) and fracture toughness (K_{IC}) of dense $MgSiN_2$-based samples.

Acknowledgements

Z. Lenčéš acknowledges the financial support by AIST, MITI, Japan, and by the Alexander von Humboldt Foundation, Germany. The work was partly supported also by the Slovak Grant Agency, project No. VEGA 2/1033. Grateful acknowledgements are due to Dr. H. Hayashi (AIST Nagoya, Japan) for the measurement of thermal diffusivity and to Dr. H. Kungl (IKM, Karlsruhe University, Germany) for the assistance during the measurement of the dielectric properties.

References

1. de With, G. and Groen, W. A., Thermal conductivity estimates for new (oxy)-nitride ceramics. In *Fourth Euro Ceramics 3, Basic Science—Optimization of Properties and Performances by Improved design and Microstructural Control*, ed. S. Mariani and V. Sergo. Gruppo Editoriale Faenza Editrice SpA, Faenza, Italy, 1995, pp. 405–412.
2. Groen, W. A., Kraan, M. J. and de With, G., Preparation, Microstructure and properties of $MgSiN_2$ ceramics. *J. Eur. Ceram. Soc.*, 1993, **12**, 413–420.
3. Davies, I. J., Uchida, H., Aizawa, M. and Itatani, K., Physical and mechanical properties of hot-pressed magnesium silicon nitride compacts with yttrium oxide addition. *Inorg. Mater. Jpn.*, 1999, **6**, 40–48.
4. Hintzen, H. T., Swaanen, P., Metselaar, R., Groen, W. A. and Kraan, M. J., Hot-pressing of $MgSiN_2$ ceramics. *J. Mater. Sci. Lett.*, 1994, **13**, 1314–1316.
5. Hintzen, H. T., Bruls, R., Kudyba, A., Groen, W. A. and Metselaar, R., Powder preparation and densification of $MgSiN_2$. In *Ceramic Transactions, Vol. 51, Int. Conf. Ceram. Proc. Sci. Tech*, ed. H. Hausner, G. L. Messing and S. Hirano. American Ceramic Society, Westerville, OH, 1995, pp. 585–589.
6. Bruls, J., Hintzen, H. T. and Metselaar, R., Preparation and characterisation of $MgSiN_2$ powders. *J. Mater. Sci.*, 1999, **34**, 4519–4531.
7. Uchida, H., Itatani, K., Aizawa, M., Howell, F. S. and Kishioka, A., Synthesis of magnesium silicon nitride by the nitridation of powders in the magnesium-silicon system. *J. Ceram. Soc. Jpn.*, 1997, **105**(11), 934–939.
8. Komeya, K., Kitagawa, I. and Meguro, T., Effect of Ca-compound addition on synthesis of AlN powder by carbothermal reduction-nitridation method. *J. Ceram. Soc. Jpn.*, 1994, **102**(7), 670–674.
9. Ide, T., Komeya, K., Meguro, T. and Tatami, J., Synthesis of AlN powder by carbothermal reduction-nitridation of various Al_2O_3 powders with CaF_2. *J. Am. Ceram. Soc.*, 1999, **82**(11), 2993–2998.
10. Uchida, H., Itatani, K., Aizawa, M. and Kishioka, A., Synthesis of magnesium silicon nitride by carbothermal reduction of magnesium silicate. *Book of Abstracts of the Annual Meeting of the Ceram. Soc. Jpn.*, 1996, 38.
11. Lenčéš, Z. Hirao, K., Yamauchi Y., Kanzaki, S., Reaction synthesis of magnesium silicon nitride powder. *J. Am. Ceram. Soc.*, 2003, **86**(7), 1088–93.
12. Niihara, K., Morena, R. and Hasselman, D. P. H., Evaluation of K_{IC} of brittle solids by the indentation method with low crack-to-indent ratios. *J. Mater. Sci. Lett.*, 1982, **1**, 13–16.
13. Sobolev, B. P. and Fedorov, X., *J. Less-Common Met.*, 1978, **60**(1), 33–46.
14. Hillert, L.. *Acta Chem. Scand.*, 1966, 290.
15. Sobolev, B. P., Fedorov, P. P., Shteynberg, D. B., Sinitsyn, B. V. and Shakhkalamian, G. S., On the problem of polymorphism and fusion of lanthanide trifluorides. I. The influence of oxygen of phase transition temperatures. *J. Solid State Chem.*, 1976, **17**(1–2), 991–999.
16. Olkhovaya, L. A., Fedorov, P. P., Ikrami, D. D. and Sobolev, B. P., *J. Therm. Anal.*, 1979, **15**(2), 355–360.
17. Tanaka, S., Itatani, K., Uchida, H., Aizawa, M., Davies, I. I.,

Suemasu, H., Nozue, A. and Okada, I., The effect of rare-earth oxide addition on the hot-pressing of magnesium silicon nitride. *J. Eur. Ceram. Soc.*, 2002, **22**, 777–783.

18. Bruls, R. J., Hintzen, H. T., de With, G., Metselaar, R. and van Miltenburg, J. C., The temperature dependence of the Grüneisen parameters of $MgSiN_2$, AlN and β-Si_3N_4. *J. Phys. Chem. Solids*, 2001, **62**, 783–792.
19. Kleebe, H.-J., Pezzotti, G., Nishida, T. and Rühle, M., Role of interface structure on mechanical properties of fluorine-doped Si_3N_4–SiC ceramics. *J. Ceram. Soc. Jpn.*, 1998, **106**, 17–24.
20. Pezzotti, G. and Ota, K., Grain-boundary sliding in fluorine-doped silicon nitride. *J. Am. Ceram. Soc.*, 1997, **80**(3), 599–603.